Motion of a skyrmionium driven by spin wave

Cite as: Appl. Phys. Lett. **112**, 062403 (2018); https://doi.org/10.1063/1.5010605
Submitted: 25 October 2017 • Accepted: 25 January 2018 • Published Online: 08 February 2018

Maokang Shen, Yue Zhang, Jun Ou-Yang, et al.

Motion of a skyrmionium driven by spin wave

Maokang Shen, Yue Zhang,[a] Jun Ou-Yang, Xiaofei Yang, and Long You
School of Optical and Electronic Information, Huazhong University of Science and Technology, Wuhan 430074, People's Republic of China

(Received 25 October 2017; accepted 25 January 2018; published online 8 February 2018)

A skyrmionium is composed of two skyrmions with opposite skyrmion numbers and different sizes in the same track. In recent years, the motion of a skyrmionium driven by spin-polarized current has been investigated. However, the motion of a skyrmionium driven by a spin wave has not been reported. In this paper, we report our work concerning the numerical analysis of spin wave-driven motion of a skyrmionium in a nanotrack. The results show that the motion of a skyrmionium was significantly influenced by varying the frequency and amplitude of the AC magnetic field for exciting a spin wave, the distance between the spin wave source and the skyrmionium, the damping coefficient of the ferromagnetic track, and the track width. We found skyrmionium deformation during its initial motion process, but its shape could be recovered as it moved farther away from the spin wave source. Additionally, a series of velocity peaks were observed in the frequency range between 25 GHz and 175 GHz. When compared to a skyrmion, the skyrmionium could be driven by a spin wave to move in a wider frequency range at a higher velocity, and the velocity of the skyrmionium kept increasing with the increase in the track width till the track edge was far away from the skyrmionium. The result offers skyrmionium potential applications in wide-frequency spintronic devices. *Published by AIP Publishing.* https://doi.org/10.1063/1.5010605

Magnetic microstructures, such as chiral domain walls and skyrmions, have been investigated widely in recent years owing to their promising applications, including novel magnetic information memory with advantages of small size, good stability, and low dissipation.[1–5]

The nontrivial topological property (skyrmion number, Q, is 1 or -1) of skyrmions leads to a skyrmion Hall effect (SkHE) that increases the risk of annihilation of skyrmions at the track edge in a racetrack memory device.[6] To resolve this problem, various designs, such as a skyrmion-based racetrack memory with edge modification,[7,8] a skyrmion-antiskyrmion bilayer,[9] and an antiferromagnetically (AFM) coupled skyrmion bilayer,[10] have been proposed. The latter two devices consist of two neighboring layers with opposite Q, resulting in the disappearance of SkHE.

In addition to the bilayers, there is another doughnut-shaped system named skyrmionium (Fig. 1). The skyrmionium equals two skyrmions with opposite Q and different sizes.[11] Since it was observed experimentally in 2013,[12] its creation, detection, and motion driven by spin-polarized current have been investigated.[13–16]

Besides spin-polarized current, spin waves can also be exploited to drive domain walls or skyrmions.[17–24] Spin wave dissipation is very low, and it can propagate in both metals and insulators, particularly in insulators with low damping, such as YIG. In theory, besides the angular momentum exchange, linear momentum exchange between skyrmions/domain walls and the spin wave may also occur. The former drags the skyrmions/domain walls to move in the opposite direction to that of spin wave propagation. In contrast, the latter pushes the skyrmions/domain walls to move in the same direction as that of spin wave propagation.[18–21,23]

Even though the spin wave-induced motion of skyrmions/domain walls has been widely reported, investigation regarding spin wave-driven motion of skyrmionium has not been found. In this paper, we report our numerical study on the skyrmionium motion induced by a spin wave. Our micromagnetic simulation was performed using the Object-Oriented MicroMagnetic Framework (OOMMF) software containing the code for the interfacial Dzyaloshinskii–Moriya interaction (DMI).[25] In our simulation, the medium was a long track with perpendicular magnetic anisotropy (PMA) (Fig. 1). The track was 2000 nm long and 1 nm thick, with the width (w) varying from 100 nm to 600 nm. We selected a cell size of 2 nm $\times$ 2 nm $\times$ 1 nm. To generate a skyrmionium and drive it by a spin wave, the medium needs to have stable PMA, suitable DMI, and small damping. The CoFeB/Pt ultrathin film satisfies the requirements. Its saturation magnetization (M_S), exchange stiffness constant (A), DMI constant (D), and anisotropy constant (K), which are close to those of Co/Pt, were 5.8×10^5 A/m, 1.5×10^{-11} J/m, 3.5 mJ/m^2, and 8×10^5 J/m^3, respectively.[26] However, the damping coefficient (α) of the

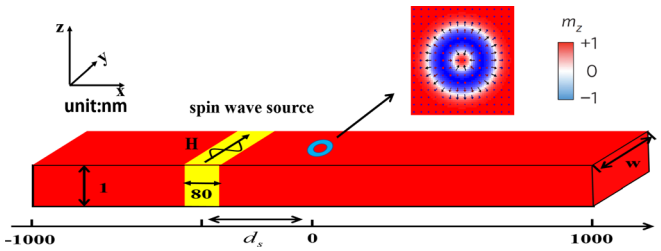

FIG. 1. Schematic of the spin wave-driven motion of a skyrmionium in a long nanotrack. The skyrmionium is composed of two skyrmions with opposite skyrmion numbers and different sizes. The skyrmionium is first generated in the middle of the track and is driven to move by a spin wave that is excited by an AC magnetic field in the yellow region on the left of the skyrmionium.

[a]Author to whom correspondence should be addressed: Yue-Zhang@hust.edu.cn

CoFeB ultrathin film can be small (0.01 or even smaller).[26–30] In the inner part of the track, α ranged between 0.005 and 0.03. To avoid spin wave reflection at the ends of the track, the α values near the two ends (50 nm long) were set to be 1.

The skyrmionium depicted in Fig. 1 was first generated in the center of the track. Initially, m_z was set to be -1 in a ring with its inner and outer radii set to be 20 nm and 40 nm, respectively. The remaining m_z in the track was set to be 1. A stable skyrmionium was finally formed after a relaxation for 4 ns.

A spin wave was excited by an AC magnetic field, $\boldsymbol{H} = H_m \sin(2\pi f t)\mathbf{e}_y$, along the y direction at a localized 80 nm long rectangle area (the yellow region in Fig. 1). The frequency (f) varied between 25 GHz and 175 GHz, the amplitude (H_m) was between 100 mT and 400 mT, and the distance between the skyrmionium and the center of the field source (d_s) was between 80 nm and 560 nm.

Snapshots of skyrmionium motion driven by the spin wave are shown in Fig. 2. In the 150 nm wide track with $\alpha = 0.005$, after a spin wave was excited ($d_s = 400$ nm) by an AC field ($f = 70$ GHz and $H_m = 400$ mT), the skyrmionium quickly moved to the right edge within 10 ns [Fig. 2(a)]. Additionally, at $t = 4$ ns, the inner red circle shifted downward, while the remaining blue part was distorted. However, the shape of the skyrmionium finally recovered when it was close to the right edge. When H_m decreased to 100 mT, the velocity of the skyrmionium was clearly reduced, and it moved to the right by around 600 nm for 40 ns [Fig. 2(b)]; when α was 0.03, the spin wave almost failed to drive the skyrmionium [Fig. 2(c)]; when f decreased to 50 GHz, the skyrmionium was destroyed [Fig. 2(d)].

The influences of f, H_m, α, and d_s on the skyrmionium motion were investigated in detail. The results shown in Fig. 3 include the temporal average x coordinate for the ring with $m_z = -1$ and a parameter, d, depicting the deformation of the skyrmionium, which was determined by

$$d = \sqrt{(x_1 - x_2)^2 + (y_1 - y_2)^2}, \tag{1}$$

where (x_1, y_1) and (x_2, y_2) are the central coordinates for the outer ring with $m_z = -1$ and the inner circle with $m_z = 1$.

As shown in Fig. 3(a), when an AC magnetic field ($f = 70$ GHz and $H_m = 400$ mT) was applied ($d_s = 400$ nm) in the 150 nm wide track, the skyrmionium was driven when α was 0.03 or smaller. In the first 10 ns, the skyrmionium

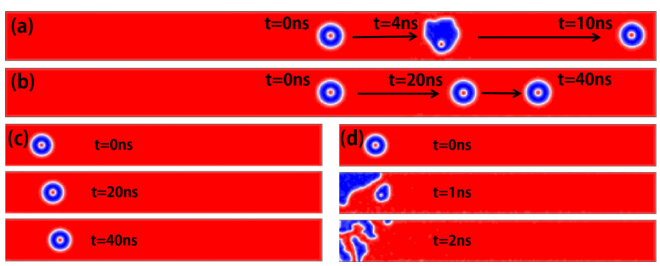

FIG. 2. Snapshots of a skyrmionium in a 150 nm wide track driven by a spin wave that was excited by an AC field under different conditions: (a) $f = 70$ GHz, $H_m = 400$ mT, $\alpha = 0.005$, and $d_s = 400$ nm; (b) $f = 70$ GHz, $H_m = 100$ mT, $\alpha = 0.005$, and $d_s = 400$ nm; (c) $f = 70$ GHz, $H_m = 400$ mT, $\alpha = 0.03$, and $d_s = 400$ nm; (d) $f = 50$ GHz, $H_m = 400$ mT, $\alpha = 0.005$, and $d_s = 400$ nm.

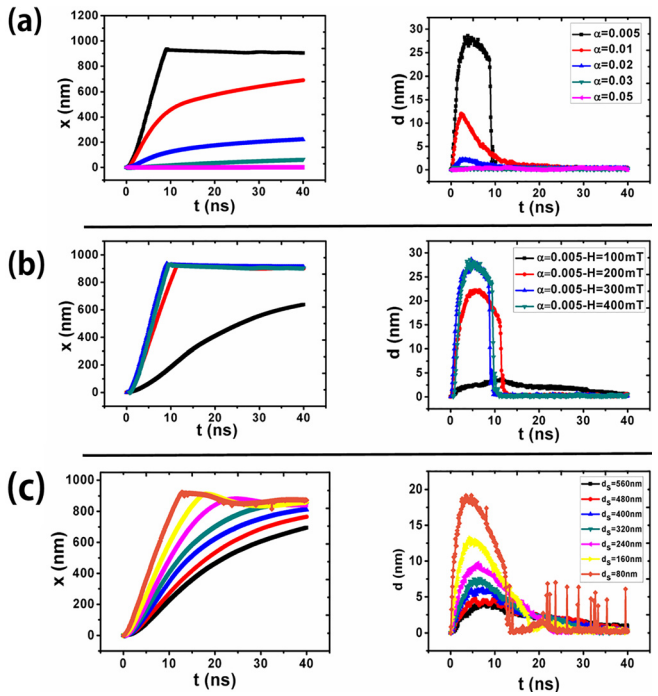

FIG. 3. The temporal average x coordinate for the skyrmionium center and the temporal parameter, d, depicting the deformation of the skyrmionium under different conditions: (a) $f = 70$ GHz, $H_m = 400$ mT, $d_s = 400$ nm, and α is in the range between 0.005 and 0.05; (b) $f = 70$ GHz, $\alpha = 0.005$, $d_s = 400$ nm, and H_m is in the range between 100 mT and 400 mT; (c) $f = 55$ GHz, $H_m = 100$ mT, $\alpha = 0.005$, and d_s is in the range between 80 nm and 560 nm.

moved fast with serious deformation. After that, the velocity was reduced and the shape recovered. In the track with $\alpha = 0.005$ and $f = 70$ GHz, the decrease in H_m from 400 mT to 100 mT reduced the velocity of the skyrmionium and suppressed the deformation [Fig. 3(b)]. The approach of the spin wave source to the skyrmionium also affected the motion of the skyrmionium [Fig. 3(c)]. When d_s decreased from 560 nm to 80 nm ($H_m = 100$ mT, $f = 55$ GHz, and $\alpha = 0.005$), the velocity clearly increased. However, the decrease in d_s also resulted in more serious deformation, especially for $d_s = 80$ nm.

Based on the above results, it was concluded that to drive a skyrmionium to move at a high speed, one should reduce α or d_s or increase H_m. Additionally, even though the net Q of a skyrmionium is zero, it is factually composed of two parts, the inner circle and the outer ring, with opposite Q. Therefore, there is still SkHE for the two regions, and they shift transversally to opposite directions under the influence of a spin wave, resulting in the deformation.[16] On the other hand, the spin wave amplitude decays with the transportation distance.[23] Therefore, skyrmionium acceleration and serious distortion occur only when it is very close to the spin wave source. When the skyrmionium is far away, both deformation and acceleration are depressed. In the case of spin current-driven skyrmionium motion, however, the skyrmionium keeps deforming and is finally converted into a single skyrmion.[16]

In addition to H_m, α, and d_s, the frequency dependence of the skyrmionium motion was also investigated. With the frequency increasing from 25 GHz to 175 GHz at an intercept of 5 GHz, several peaks for the average velocity over

the 40 ns timeframe were observed (Fig. 4). In the 150 nm and 200 nm wide track ($\alpha = 0.005$), when H_m was 100 mT, an abrupt velocity jump occurred at 55 GHz and the strongest peaks appeared near 80 GHz with other weaker peaks found at 115 GHz and 165 GHz. In the narrowest track ($w = 100$ nm), when H_m was 100 mT, the main-peak velocity (v_{max}) at 80 GHz is smaller than that in the 150 nm and 200 nm wide track due to the pinning effect from the track edge. However, the velocity peaks in the 100 nm wide track also appeared at 50 GHz, 75 GHz, 115 GHz, and 165 GHz. A similar phenomenon has also been discovered in domain walls, vortex walls, and skyrmion motion driven by a spin wave.[18,21,22,31–33] These discrete frequencies for the maximum velocity may be attributed to internal oscillation modes of a skyrmionium and can be related to the variation of the amplitude of the spin wave.[33]

As a comparison, we investigated the frequency-dependent motion of a skyrmion in the track under the same conditions. In the 100 nm wide track, the frequencies of velocity peaks of the skyrmion are consistent with those of skyrmionium. However, the velocities at higher frequencies ($f > 100$ GHz) were considerably smaller than those of the skyrmionium. In the 150 nm wide track, the skyrmion velocities were significantly lower than those of the skyrmionium, and when the frequency was greater than 100 GHz, the skyrmion was not able to be driven. In the 200 nm wide track, small negative velocities were even observed around 50 GHz. Therefore, with respect to the skyrmion, the skyrmionium could be driven to move at a higher speed in a wider frequency range.

The w-dependence of the motion of the skyrmionium was also investigated. One can see that v_{max} increased with the increase in w from 100 nm to 300 nm. When w was larger than 300 nm, v_{max} was reduced [Fig. 4(d)]. It is interesting that both the inner (R_1) and outer (R_2) radii of the skyrmionium also increased with w varying from 100 nm to 300 nm (the inset), and they became constant at a larger w. This result means that when w was 300 nm or smaller, the size of the skyrmionium was restricted by the track edge; when the width was larger, the track edge was far away and the skyrmionium became stable finally ($R_1 = 9$ nm and $R_2 = 39$ nm).

To study the mechanism of the dependence of velocity on the track width, we have recorded the temporal m_y at $x = -201$ nm and $x = 201$ nm. As shown in Fig. 5, in the tracks containing skyrmions, the variation of the track width made a great impact on temporal m_y. When the track width was 100 nm, the amplitude of oscillation of m_y ($A(m_y)$) at $x = 201$ nm was much smaller than that at $x = -201$ nm. In the 150 nm wide track, $A(m_y)$ at $x = 201$ nm was clearly enhanced when compared to that in the 100 nm wide track. When $w = 200$ nm, $A(m_y)$ at $x = 201$ nm became even larger than that at $x = -201$ nm. These results indicate that in the 100 nm wide track, the transmission of the spin wave through the skyrmion is inhibited, but in the 200 nm wide track, the spin wave is easy to pass the skyrmion region. Additionally, a slow increase of $A(m_y)$ was seen at $x = -201$ nm, which may indicate a small reflection of the spin wave. In general, the transmission of the spin wave through a skyrmion/domain wall drags the skyrmion to move in the opposite direction to the spin wave propagation due to the STT effect (the exchange of angular momentum). In contrast, the reflection of the spin wave pushes the skyrmion/domain wall to move in the same direction as that of spin wave propagation due to the exchange of momentum.[20,21,23,31–33] The increase in the track width enhances the transmission of the spin wave, which reduces the velocity of skyrmion to be negative. However, in the three tracks containing skyrmionium, the m_y values at $x = 201$ nm were all smaller than those at $x = -201$ nm. $A(m_y)$ varied periodically at $x = -201$ nm. At $x = 201$ nm, $A(m_y)$ also varied with time. These results indicate that the reflection of the spin wave by the moving skyrmionium remained dominant over the transmission of the spin wave with the increase in the track width from 100 nm to 200 nm. As a result, the skyrmionium was pushed to move

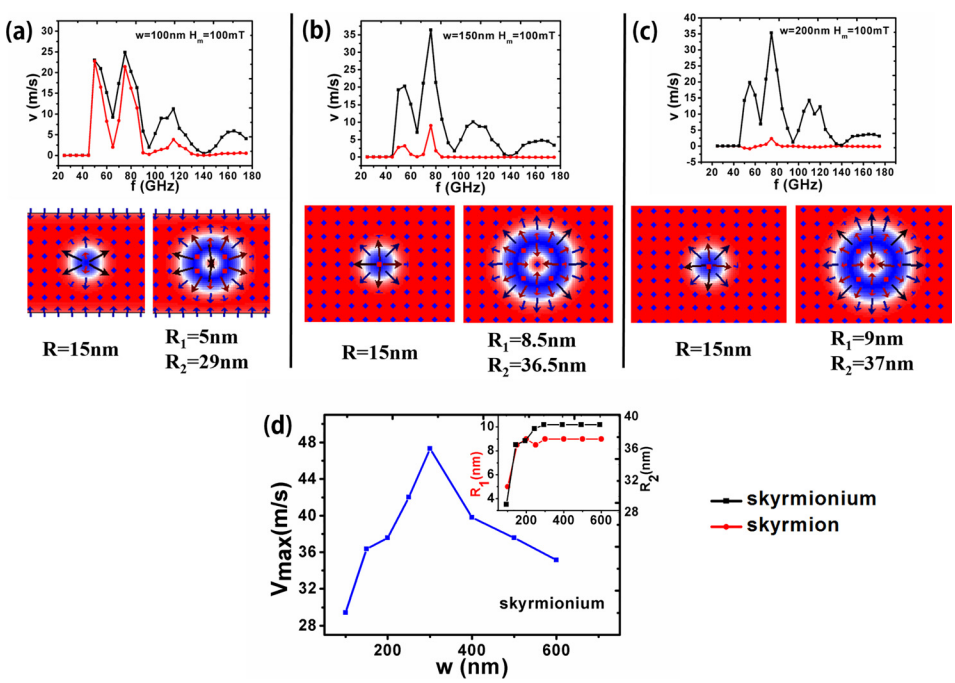

FIG. 4. In the first line: The frequency dependence of the average skyrmion and skyrmionium velocities driven by the spin wave ($H_m = 100$ mT, $d_s = 400$ nm, and $\alpha = 0.005$) in the tracks with different widths: (a) $w = 100$ nm, (b) $w = 150$ nm, and (c) $w = 200$ nm. In the second line: The radius of skyrmions and the inner and outer radii of skyrmionium in the tracks with different widths. In the third line: The track width dependence of the average velocity for the peak around 75 GHz (v_{max}). The inset shows the track width dependence of the inner and outer radii of skyrmionium.

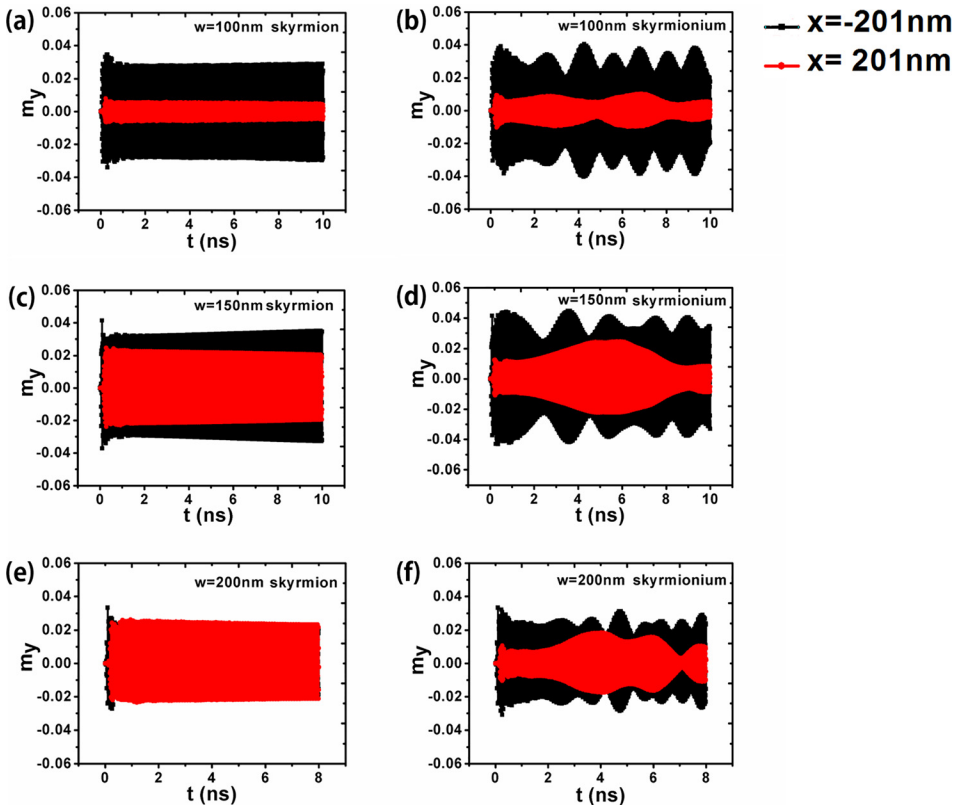

FIG. 5. The oscillation of m_y at $x = -201$ nm and $x = 201$ nm in the tracks with different widths: (a) $w = 100$ nm for the skyrmion, (b) $w = 100$ nm for the skyrmionium, (c) $w = 150$ nm for the skyrmion, (d) $w = 150$ nm for the skyrmionium, (e) $w = 200$ nm for the skyrmion, and (f) $w = 200$ nm for the skyrmionium. The frequency of the ac field for the exciting spin wave is 110 GHz.

by the spin wave at a higher speed. However, when w was larger than 300 nm, the size of the skyrmionium did not change with the increase in w. As a result, the area for the transmission of the spin wave between the skyrmionium and the track edge was enlarged, leading to the easier transmission of the spin wave and the decrease in the velocity of the skyrmionium.

In summary, skyrmionium motion driven by a spin wave was investigated using micromagnetic simulation. Skyrmionium velocity and deformation can be effectively manipulated by changing the amplitude and frequency of the external AC magnetic field, damping coefficient, track width, and distance between the spin wave source and the skyrmionium. The velocity peaks were observed at a series of discrete frequencies between 25 GHz and 175 GHz. When compared to the skyrmion, the skyrmionium could be driven to move by the spin wave in a wider frequency and track width range and at higher speeds. When the track width was between 100 and 200 nm, the transmission of the spin wave through the skyrmion was enhanced, while the reflection kept dominant over the transmission for the skyrmionium. As a result, the velocity of the skyrmion was greatly reduced, but that of skyrmionium increased. The increase in the velocity of the skyrmionium occurred when its size kept increasing with the increase in the track width from 100 nm to 300 nm. When the track width was larger, the size of the skyrmionium became stable due to the weakened edge effect and the velocity of the skyrmionium was reduced.

The authors would like to acknowledge the financial support from the National Natural Science Foundation of China (Nos. 11574096 and 61674062) and Huazhong University of Science and Technology (No. 2017KFYXJJ037).

[1]S. H. Yang and S. Parkin, J. Phys.: Condens. Matter **29**, 303001 (2017).
[2]G. Finocchio, F. Büttner, R. Tomasello, M. Carpentieri, and M. Kläui, J. Phys. D: Appl. Phys. **49**, 423001 (2016).
[3]W. Kang, Y. Huang, X. Zhang, Y. Zhou, and W. Zhao, Proc. IEEE **104**, 2040 (2016).
[4]W. Jiang, G. Chen, K. Liu, J. Zang, S. G. E. te Velthuis, and A. Hoffmann, Phys. Rep. **704**, 1 (2017).
[5]N. Nagaosa and Y. Tokura, Nat. Nanotechnol. **8**, 899 (2013).
[6]W. Jiang, X. Zhang, G. Yu, W. Zhang, X. Wang, M. B. Jungfleisch, J. E. Pearson, X. Cheng, O. Heinonen, K. L. Wang, Y. Zhou, A. Hoffmann, and S. G. E. te Velthuis, Nat. Phys. **13**, 162 (2017).
[7]I. Purnama, W. L. Gan, D. W. Wong, and W. S. Lew, Sci. Rep. **5**, 10620 (2015).
[8]Y. Zhang, S. Luo, B. Yan, J. Ou-Yang, X. Yang, S. Chen, B. Zhu, and L. You, Nanoscale **9**, 10212 (2017).
[9]S. Huang, C. Zhou, G. Chen, H. Shen, A. K. Schmid, K. Liu, and Y. Wu, Phys. Rev. B **96**, 144412 (2017).
[10]X. Zhang, Y. Zhou, and M. Ezawa, Nat. Commun. **7**, 10293 (2016).
[11]A. Bogdanov and A. Hubert, J. Magn. Magn. Mater. **195**, 182 (1999).
[12]M. Finazzi, M. Savoini, A. R. Khorsand, A. Tsukamoto, A. Itoh, L. Duo, A. Kirilyuk, T. Rasing, and M. Ezawa, Phys. Rev. Lett. **110**, 177205 (2013).
[13]S. Komineas and N. Papanicolaou, Phys. Rev. B **92**, 174405 (2015).
[14]S. Komineas and N. Papanicolaou, Phys. Rev. B **92**, 064412 (2015).
[15]H. Fujita and M. Sato, Phys. Rev. B **95**, 054421 (2017).
[16]X. Zhang, J. Xia, Y. Zhou, D. Wang, X. Liu, W. Zhao, and M. Ezawa, Phys. Rev. B **94**, 094420 (2016).
[17]X. Zhang, M. Ezawa, D. Xiao, G. P. Zhao, Y. Liu, and Y. Zhou, Nanotechnology **26**, 225701 (2015).
[18]J. Ding, X. Yang, and T. Zhu, IEEE Trans. Magn. **51**(11), 1500504 (2015).
[19]Y. Liu, G. Yin, J. Zang, J. Shi, and R. K. Lake, Appl. Phys. Lett. **107**, 152411 (2015).
[20]J. Iwasaki, A. J. Beekman, and N. Nagaosa, Phys. Rev. B **89**, 064412 (2014).
[21]X. Wang, G. Guo, Y. Nie, G. Zhang, and Z. Li, Phys. Rev. B **86**, 054445 (2012).
[22]D. Han, S. Kim, J. Lee, S. J. Hermsdoerfer, H. Schultheiss, B. Leven, and B. Hillebrands, Appl. Phys. Lett. **94**, 112502 (2009).
[23]W. Wang, M. Albert, M. Beg, M. A. Bisotti, D. Chernyshenko, D. Cortes-Ortuno, I. Hawke, and H. Fangohr, Phys. Rev. Lett. **114**, 087203 (2015).
[24]J. Xia, Y. Huang, X. Zhang, W. Kang, C. Zheng, X. Liu, W. Zhao, and Y. Zhou, J. Appl. Phys. **122**, 153901 (2017).
[25]S. Rohart and A. Thiaville, Phys. Rev. B **88**, 184422 (2013).

[26]J. Sampaio, V. Cros, S. Rohart, A. Thiaville, and A. Fert, Nat. Nanotechnol. **8**, 839 (2013).
[27]S. Iihama, S. Mizukami, H. Naganuma, M. Oogane, Y. Ando, and T. Miyazaki, Phys. Rev. B **89**, 174416 (2014).
[28]T. Devolder, P.-H. Ducrot, J.-P. Adam, I. Barisic, N. Vernier, Joo-Von Kim, B. Ockert, and D. Ravelosona, Appl. Phys. Lett. **102**, 022407 (2013).
[29]X. Liu, W. Zhang, M. J. Carter, and G. Xiao, J. Appl. Phys. **110**, 033910 (2011).
[30]A. Natarajarathinam, Z. R. Tadisina, T. Mewes, S. Watts, E. Chen, and S. Gupta, J. Appl. Phys. **112**, 053909 (2012).
[31]P. Yan, X. S. Wang, and X. R. Wang, Phys. Rev. Lett. **107**, 177207 (2011).
[32]J.-S. Kim, M. Stärk, M. Kläui, J. Yoon, C.-Y. You, L. Lopez-Diaz, and E. Martinez, Phys. Rev. B **85**, 174428 (2012).
[33]S.-M. Seo, H.-W. Lee, H. Kohno, and K.-J. Lee, Appl. Phys. Lett. **98**, 012514 (2011).